

Interchange instability at the leading part of reconnection jets

M. S. Nakamura and H. Matsumoto

Radio Science Center for Space & Atmosphere, Kyoto University, Japan

M. Fujimoto

Department of Earth and Planetary Sciences, Tokyo Institute of Technology, Japan

Received 16 July 2001; revised 22 September 2001; accepted 13 November 2001; published 27 April 2002.

[1] Three-dimensional structures of reconnection jets are investigated by hybrid simulations. Magnetic reconnection is initiated by ad-hoc anomalous resistivity, which is uniform in the cross-tail direction but localized within the meridian plane. At the interface between the reconnection jet and the pre-existing plasma sheet ahead of it, the reconnected field lines are piled up and the plasma density is enhanced by compression. The interface becomes unstable to an interchange instability and deforms itself into a wavy shape. In the non-linear growth phase, the wavy perturbations grow into magnetic bubbles into which the field lines are converged and the bubbles move faster than the other parts. It is suggested that this instability can generate localized channels with a cross-tail extent of a few R_E , in which plasma and magnetic field transports are achieved, and thus may well be related to the formation of the bursty bulk flows in the magnetotail. **INDEX TERMS:** 7835 Space Plasma Physics: Magnetic reconnection; 2744 Magnetospheric Physics: Magnetospheric configuration and dynamics; 2772 Magnetospheric Physics: Plasma waves and instabilities; 7843 Space Plasma Physics: Numerical simulation studies

1. Introduction

[2] Magnetic reconnection is one of the most important processes in the space, astronomical, and laboratory plasmas, not only changing topology of magnetic field lines but also generating fast and hot plasma flows by converting magnetic energy into plasma kinetic and thermal energies. In the magnetotail, magnetic reconnection is considered to work as an engine for plasma, magnetic field, and energy transports at substorms. Earthward localized fast plasma flows, so called bursty bulk flows (BBFs), are frequently observed in the near-Earth magnetotail and are considered to be consequences of magnetic reconnection [Angelopoulos *et al.*, 1992]. The BBFs have a cross-tail extent of order of 3 R_E or less [Angelopoulos *et al.*, 1997] and are related with local auroral activities [Sergeev *et al.*, 2000]. These suggest that reconnection jets in the near-Earth magnetotail have an intrinsic 3-D structure within which the transient and localized transports are attained. Not only such a small scale of the BBFs but also recent observational studies revealing the significance of ion kinetic effects in the magnetotail reconnection jets [Fujimoto *et al.*, 1996].

[3] Recently, Pritchett *et al.* [1997] and Pritchett and Coroniti [2000] have performed a series of 3-D electromagnetic particle simulations starting from a kinetic 2-D tail-like equilibrium superposed a line dipole field, in which the external convection electric field is applied to the simulation domain. They have suggested that the earthward convective flow becomes localized by an interchange mode driven by a tailward gradient in the equatorial magnetic field. On the other hand, Chen and Wolf

[1993, 1999] have proposed the plasma bubble model that the localized underpopulated plasma tubes are accelerated earthward as BBFs. This model well agrees with the plasma-depleted BBFs [Sergeev *et al.*, 1996, 2000] but is not sure to be appropriate for the other BBFs, while it is still ambiguous what mechanism gives the seeds of the localized underpopulated plasma tubes in the magnetotail.

[4] In this paper, we have performed large-scale 3-D hybrid simulations to demonstrate that the reconnection jet uniformly initiated in the cross-tail direction develops into a localized jet structure by an interchange instability even in the simplest 1-D plasma sheet model [Nakamura *et al.*, 2001]. Here, we investigate the instability with attention to the 3-D structure in the non-linear phase. The magnetic bubbles at the leading part of the reconnection jet, which is the cross-section of the magnetic flux bundles at the equatorial plane, have a cross-tail extent of a few R_E and is associated with a sausage-like structure on the cross-tail section. It is also shown that the wavelength of the instability, or the dawn-dusk scale of the bubble, is rather insensitive to the initial plasma sheet thickness.

2. Simulation Model and Results

[5] The 3-D hybrid simulation used here is the same as before [Nakamura and Fujimoto, 1998, 2000; Nakamura *et al.*, 2001]. Here the conventional coordinates system, the x -, y -, and z -axis directed earthward, duskward, and northward, respectively, are used. Hereinafter, simulation results are normalized as follows: Magnetic field by B_0 (lobe magnetic field), plasma density by n_0 (lobe density), velocity by V_A (the Alfvén velocity in the lobe), time scale by Ω_i^{-1} (the inverse of the ion cyclotron frequency in the lobe), spatial scale by $\rho_i = V_A \Omega_i^{-1}$, and magnitude of the resistivity by $\mu_0 \rho_i V_A$, respectively. With typical values, i.e., the lobe density of 0.05 particle/cm³ and the lobe magnetic field of 20 nT, the unit time and spatial scales are $\Omega_i^{-1} \simeq 0.5$ s and $\rho_i \simeq 1000$ km, respectively. Since the symmetric boundary condition is assumed in the x and z directions and the periodic boundary condition is assumed in the y direction, calculations are done only the first quadrant of the whole domain, that is, $0 \leq x \leq L_x$, $0 \leq y \leq L_y$, and $0 \leq z \leq L_z$ (L_x , L_y , and L_z are listed in Table 1). The cell size is $\Delta x = \Delta y = 0.8$ (0.6 for Run 5) and $\Delta z = 0.5$ (0.3 for Run 5). We use the 1-D Harris equilibrium as the initial plasma sheet $\mathbf{B} = [B_x(z)0, 0]$, where $B_x(z) = B_0 \tanh(z/D)$ for $0 \leq z < L_z/2$. Another current sheet is added, $B_x(z) = -B_0 \tanh((z - L_z)/D)$ for $L_z/2 \leq z \leq L_z$, for ease of the boundary condition. D is the half-thickness of the initial plasma sheet. Cold ions are uniformly distributed as the background lobe population. Sixty-four ion particles in a cell represent unit density. The plasma sheet ions are modeled by a drifting Maxwellian distribution, whose peak density at the central plasma sheet is 2 in the normalized unit. Electrons are initially at rest and their temperature is fixed to zero for simplicity. Anomalous resistivity has a peak at the $x = z = 0$ corner of the simulation box, $\eta(x, z) = \eta_0 [\exp(-(x/k_x)^2 - (z/k_z)^2) + 0.01]$, where $\eta_0 = D$ and $k_x = k_z = D$. Note that the shape of the

Table 1. Initial Configurations and Results

Run	D	$L_x \times L_y \times L_z$	Mode	λ
1	2	$320 \times 160 \times 64$	10	16
2	3	$320 \times 56 \times 32$	2	28
3	4	$320 \times 80 \times 40$	3	26.7
4	6	$320 \times 80 \times 40$	3	26.7
5	1.5	$240 \times 60 \times 24$	4	15

resistivity η is invariant in the y direction. Since the symmetric boundary condition in the z direction allows the growth of neither the tail-KH instability [Nakamura and Fujimoto, 2000] nor the current sheet breakup [Arzner and Scholer, 2001], their effects are out of the scope of this paper. Since the simulation box is relatively large, the rarefaction in the lobe above the reconnection region could have a little influence on the reconnection rate and the reconnection jet velocity in the later phase.

[6] Figure 1 shows temporal development of B_z at the central plasma sheet ($z = 0$ plane) from $T = 80$ to $T = 360$ in Run 1. These are plotted by looking down onto the central plasma sheet from the north ($z > 0$) and moving earthward at $V_x = 0.5$. The parts of the simulation domain including the leading part of the reconnection jet are shown. At $T = 80$, both B_z and plasma density (not shown)

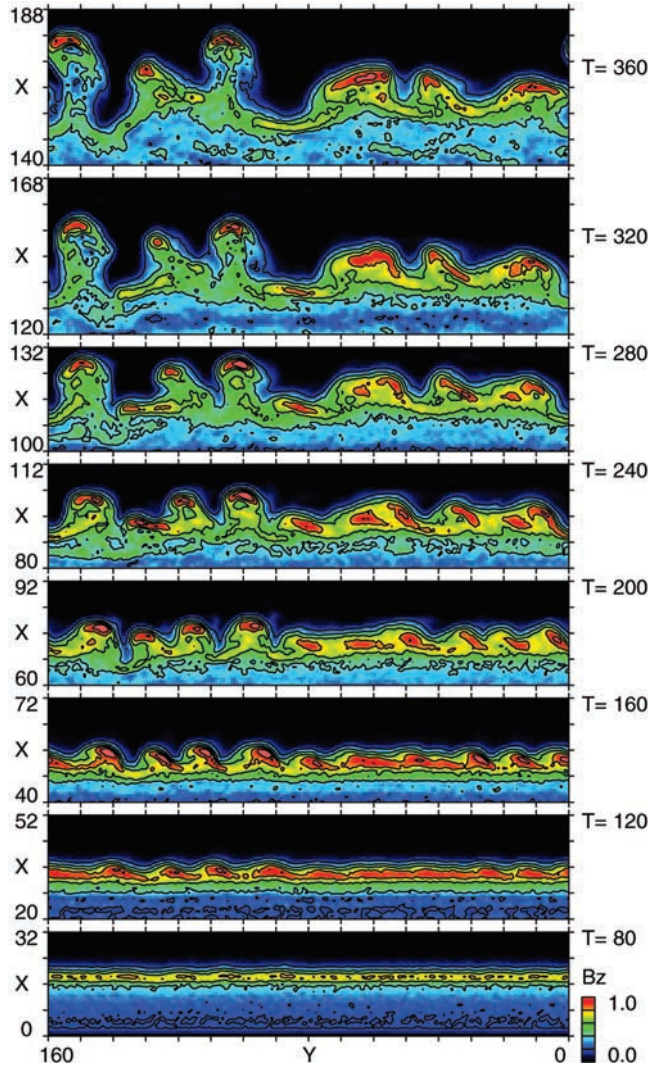


Figure 1. The B_z plots on the central plasma sheet ($z = 0$ plane) from $T = 80$ to $T = 360$ in Run 1. The leading part of the reconnection jet is shown.

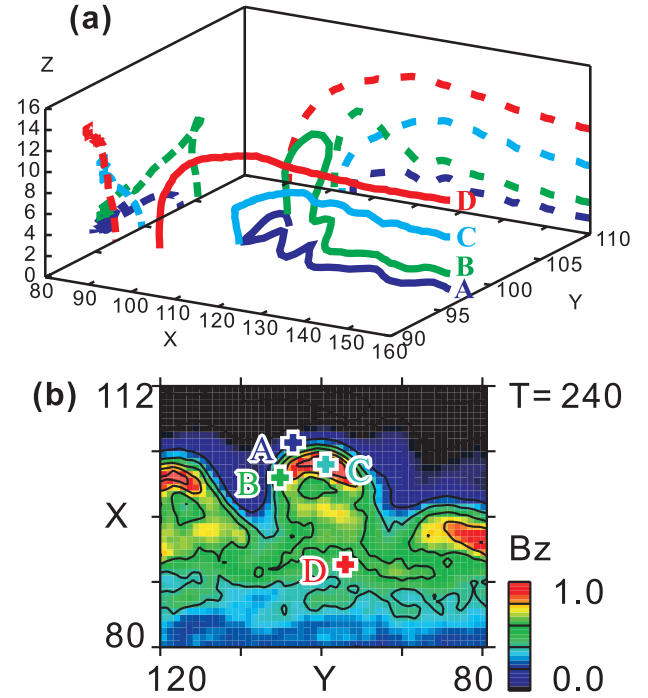


Figure 2. (a) The three-dimensional display of four magnetic field lines at $T = 240$. (b) The foot-points of the four field lines are superposed on the B_z plot at the central plasma sheet.

are enhanced by compression around the interface between the reconnection jet and the pre-existing plasma sheet. The peak of B_z is located slightly behind the plasma density peak. At $T = 120$, islands of B_z enhancement (mode 10, wavelength $\lambda \sim 16$) at the interface are emerging. The leading part of the reconnection jet becomes warped and eventually comes to show a bubble-like structure which is typical of the interchange instabilities after $T = 160$. Substantial magnetic field lines reconnected at the early stage are converging into the magnetic bubbles. The magnetic bubbles are accelerated earthward and move faster than the other parts of the reconnection jet front. They also shift duskward slowly. Furthermore, after $T = 240$, some pairs are merging into larger bubbles.

[7] To investigate the 3-D structure of the reconnection jet front, we give attention to one of the magnetic bubbles around $(x, y) = (100, 100)$ at $T = 240$. Figure 2a shows a 3-D display of magnetic field lines traced from 4 points at $(x, y) = (160, 96)$ with different z values of 1.5, 3.0, 6.5, and 10.0. Different field lines are depicted by different colors. In addition to the 3-D display of the field lines, their projections onto the x - z and y - z planes are plotted together by dotted lines of the same colors. The difference in the z value represents the difference in the time when the field lines are reconnected, i.e., the smaller z value indicates the earlier experience of reconnection. The field lines are traced until they reach the central plasma sheet and their foot-points are superposed on the B_z plot at the central plasma sheet in Figure 2b. In Figure 2a, A (dark blue) is the field line that reconnected earliest of all and has the foot-point at the front edge of the magnetic bubble. It is bent sharply duskward just ahead of the magnetic bubble because of the electron motions, to which field lines are frozen, following the localized fast duskward drifting ion motions to adjust the local current. The bended field lines around the leading edge of the reconnection jet are also observed in the 2-D and 3-D hybrid simulations [Nakamura et al., 1997; Nakamura and Fujimoto, 1998]. An Alfvén wave-like signature is evident in the shape of the field lines A and B and indicates the perturbative action of the leading part of the reconnection jet due to the instability.

[8] To understand the shapes of the field lines B, C, and D better, we show, in Figure 3, the B_x and plasma density plots at $x = 104$ cross-tail plane, which is located just ahead of the bubble. The lower halves ($z < 0$) are added in these plots for convenience. The points where the field lines B, C, and D thread this plane are marked by the crosses. In the non-linear phase when the bubbles form, a good correlation of the plasma density enhancement with the B_z enhancement is lost at the reconnection jet front. The faster moving bubbles thrust aside the pre-existing plasma sheet and gather the plasma beside them. The plasma sheet expands in the north-south direction between the bubbles. This expansion of the plasma sheet generates complicated 3-D shapes of the magnetic field lines as depicted by the field line B (green). The field line B is deflected duskward from the bubble location and whips northward while it wraps around the high-density region. Then, it dives down into the central plasma sheet at the flank of the bubble. The field line C (light blue) has a foot-point in the middle of the bubble. It hardly expands northward and is just curved a little duskward. This, together with A (dark blue) and B (green), indicates that the pre-existing plasma sheet almost keeps its initial thickness in the fore-bubble region but expands in the north-south direction between the bubbles as seen a sausage-like structure in the density plot. The field line D (red) is the field line that reconnected at the later stage and does not have the foot-point in the bubble. It is hardly influenced by the development of the bubbles. That means that the field lines, which have reconnected in the later stage and do not reach the leading part of the reconnection jet, are almost uniform in the dawn-dusk direction.

[9] Now we change the initial current sheet thickness D and study how it controls the wavelength of the instability. Figure 4 shows the results for $D = 1.5 \sim 6$ in Table 1. The circles represent the wavelength of the most growing mode calculated by dividing L_y by the mode number. The crosses represent the wavelengths when the mode numbers are increased or decreased by one from the most growing one. Because of the limited spatial extent L_y , the exact fastest growing wavelengths are not obtained but they will come between the two crosses. The figure indicates that the unstable wavelength is not scaled linearly to the initial plasma sheet thickness, but stays at a few tens ion inertial scale for $D > 2$. The results suggest that ion inertia effects or the ion Larmor radius effects play significant roles, even when the thickness of the plasma sheet ($2D$) is 12 times as large as the ion inertia length when the MHD description is expected to be reasonably good.

3. Discussions

[10] We have presented simulation results of the interchange instability at the leading part of reconnection jet. The instability generates magnetic bubbles on the equatorial plane and a sausage-like structure on the cross-tail section. *Dahlburg et al.* [1992] observed that the 3-D secondary instability of the 2-D quasi-steady saturated tearing reconnection layer appears in 3-D MHD simulations of reconnection. Their discussion on the energetics of the instability as well as the other interchange instabilities, for instance the ballooning instability having a configuration partially similar to

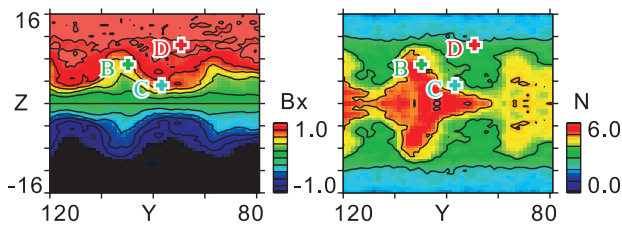


Figure 3. The B_x and plasma density plots at the $x = 104$ cross-tail plane at $T = 240$. The points that the field lines B, C, and D thread this plane are superposed in these figures.

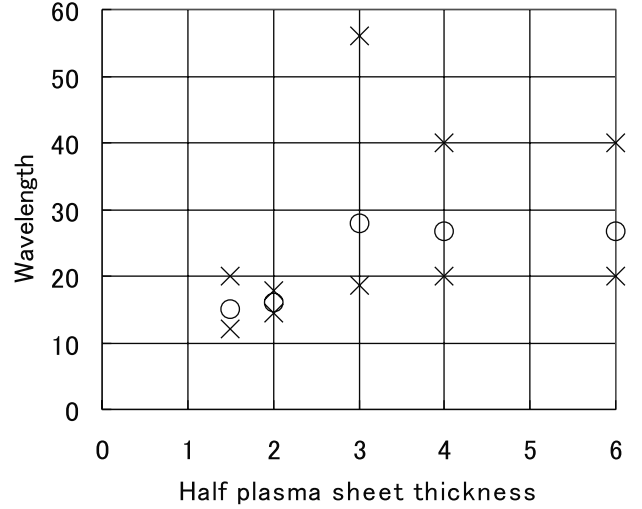


Figure 4. The wavelength of the instability plotted versus the initial plasma sheet half-thickness D . The circles show the fastest growing wavelength obtained in the simulations. The crosses show the wavelengths calculated by increasing or decreasing the mode number by one from the fastest growing one.

the observed one and the 2-D Richtmyer-Meshkov (a member of the interchange instability family) instability considered at the equatorial plane, is useful to understand the properties of the interchange instability at the reconnection jet front. However, because it is the instability, non-linearly driven from a 3-D non-equilibrium state, pinning down its nature is still tough and under way. We have found that the instability exists in MHD as well as in Hall-MHD system. In these fluid systems, the instability behaves quite similarly to the Richtmyer-Meshkov instability with the shortest wavelength that is allowed in the simulation to develop faster [*TanDokoro et al.*, in preparation]. As such, the locking of the wavelength seen in Figure 4 is likely to be due to the finite ion Larmor radius effects.

[11] The instability will also show up when the dawn-dusk extent of the reconnection line is larger than the unstable wavelength. When this condition is met, the instability will generate localized channels of a few R_E wide in the geomagnetotail, in which fluxes of plasma, magnetic field, and energy are concentrated. This may well be consistent with the formation of the BBFs observed in the near-Earth magnetotail [*Angelopoulos et al.*, 1992, 1997]. The present results show that the localized flow channels can be generated even if starting from the simplest 1-D thin plasma sheet not like the previous works assuming a 2-D magnetotail-like equilibrium. The instability may possibly give the seeds of the localized underpopulated plasma tubes in the plasma bubbles model in the distant tail reconnection [*Chen and Wolf*, 1993, 1999]. However, since a lot of simplifications are introduced in order to concentrate on the nature of the instability, more realistic setting-up is necessary to do a comparative study with observations. The most crucial issue would be to start from a 2-D magnetotail-like equilibrium, which is being carried out.

[12] **Acknowledgments.** This work was supported by Simulation Promotion Program of STEL, Nagoya University. Computations were performed at Nagoya University Computation Center and the KDK system of RASC, Kyoto University as a collaborative research project.

References

- Angelopoulos, V., et al., Bursty Bulk Flows in the Inner Central Plasma Sheet, *J. Geophys. Res.*, 97, 4027–4039, 1992.
- Angelopoulos, V., et al., Magnetotail flow bursts: Association to global magnetospheric circulation, relationship to ionospheric activity, and di-

- rect evidence for localization, *Geophys. Res. Lett.*, **24**, 2271–2274, 1997.
- Arzner, K., and M. Scholer, Kinetic structure of the psot plasmoid plasma sheet during magnetotail reconnection, *J. Geophys. Res.*, **106**, 3827–3844, 2001.
- Chen, C. X., and R. A. Wolf, Interpretation of high-speed flows in the plasma sheet, *J. Geophys. Res.*, **98**, 21,409–21,419, 1993.
- Chen, C. X., and R. A. Wolf, Theory of thin-filament motion in Earth's magnetotail and its application to bursty bulk flows, *J. Geophys. Res.*, **104**, 14,613–14,626, 1999.
- Dahlburg, R. B., S. K. Antiochos, and T. A. Zang, Secondary instability in three-dimensional magnetic reconnection, *Phys. Fluids B*, **4**, 3902–3914, 1992.
- Fujimoto, M., M. S. Nakamura, T. Nagai, T. Mukai, T. Yamamoto, and S. Kokubun, New kinetic evidence for the near-Earth reconnection, *Geophys. Res. Lett.*, **23**, 2533–2536, 1996.
- Nakamura, M. S., and M. Fujimoto, A three-dimensional hybrid simulation of magnetic reconnection, *Geophys. Res. Lett.*, **25**, 2917–2920, 1998.
- Nakamura, M. S., and M. Fujimoto, 3-D hybrid simulation of magnetic reconnection in a thin current sheet, *Adv. Space Res.*, **26**, 431–434, 2000.
- Nakamura, M. S., M. Fujimoto, and K. Maezawa, Ion dynamics and resultant velocity space distributions in the course of magnetotail reconnection, *J. Geophys. Res.*, **103**, 4531–4546, 1997.
- Nakamura, M. S., M. Fujimoto and H. Matsumoto, Instability at interface between reconnection jet and pre-existing plasma sheet, *Adv. Space Res.*, in press, 2001.
- Pritchett, P. L., and F. V. Coroniti, Localized convection flows and field-aligned current generation in a kinetic model of the near-Earth plasma sheet, *Geophys. Res. Lett.*, **27**, 3161–3164, 2000.
- Pritchett, P. L., F. V. Coroniti, and R. Pellat, Convection-driven reconnection and the stability of the near-Earth plasma sheet, *Geophys. Res. Lett.*, **24**, 873–876, 1997.
- Sergeev, V. A., et al., Detection of localized, plasma-depleted flux tubes or bubbles in the midtail plasma sheet, *J. Geophys. Res.*, **101**, 10,817–10,826, 1996.
- Sergeev, V. A., et al., Multiple-spacecraft observation of a narrow transient plasma jet in the Earth's plasma sheet, *Geophys. Res. Lett.*, **27**, 851–854, 2000.

M. S. Nakamura and H. Matsumoto, Radio Science Center for Space and Atmosphere, Kyoto University, Uji 611-0011, Japan. (msn@kurasc.kyoto-u.ac.jp; matsumot@kurasc.kyoto-u.ac.jp)

M. Fujimoto, Department of Earth and Planetary Sciences, Tokyo Institute of Technology, Tokyo 152-8551, Japan. (fujimoto@geo.titech.ac.jp)